特集　造血器腫瘍に対する新規治療薬開発の現状と臨床応用の可能性

放射性同位元素標識抗CD20抗体*

飛内賢正**

Key Words：radioimmunotherapy, radioimmunoconjugate, CD20, B-cell lymphoma, ibritumomab tiuxetan

はじめに

Hybridoma法によるマウスモノクローナル抗体(monoclonal antibody；mAb)作製法が開発されて約30年，mAbによるヒト悪性腫瘍の治療研究が開始されて約25年が経過した．マウスmAb療法には，異種抗体(human anti-murine antibody；HAMA)産生や，抗免疫グロブリンidiotype抗体療法中の体細胞突然変異によるBリンパ腫細胞のidiotypic changeによるescapeなどの種々の問題が存在した．しかし，新しいtechnology導入が継続され，①キメラ抗体・ヒト化抗体，②毒素や抗がん剤を抱合したimmunotoxin, chemoimmunoconjugate，③放射性同位元素を標識したradioimmunoconjugateの3つの突破口の有効性が明らかになった．

本稿では，臨床的有用性が確認されたキメラ型抗CD20抗体rituximab[1)2)]の次世代のB細胞リンパ腫の抗体医薬として注目を集めている放射性同位元素標識抗CD20抗体の国内外の臨床開発の現状を紹介する．

抗体療法の標的抗原

B細胞リンパ腫に対する抗体療法の標的抗原としてこれまでに検討されてきたのは細胞表面免疫グロブリンidiotype, CD19, CD20, CD21, CD22, CD37, CD52, HLA-DRなどである．CD19とCD22は特異抗体が反応すると細胞表面の抗原抗体複合体が細胞内に取り込まれる性質を有するため，immunotoxinもしくはchemoimmunoconjugateの標的抗原としても研究の対象とされてきた．

Radioimmunotherapyの標的抗原としては，抗体と反応した際にmodulateせず，細胞内に取り込まれない抗原が有利とされる．B細胞リンパ腫に対するradioimmunotherapyの標的抗原として検討されてきたのはCD20, CD22, HLA-DRなどであるが，もっとも精力的に臨床試験が展開されているのは抗CD20 radioimmunoconjugateである．

CD20抗原は正常B細胞と大半のBリンパ腫細胞に発現し，他の体細胞に発現していない，特異性のきわめて高い白血球分化抗原である．図1にCD20抗原の模式図を示す．

Radioimmunotherapyの基本原理

悪性リンパ腫の腫瘍細胞は本来放射線治療に感受性が高い．非抱合型抗体やimmunotoxin, chemoimmunoconjugateと異なり，radioimmunoconjugateは標的抗原を発現していない隣接した腫瘍細胞にも殺細胞効果を発揮し，血管形成の乏しい腫瘤性病変に対する効果(bystander effect

* Radioimmunotherapy of B-cell lymphoma with anti-CD20 radioimmunoconjugates.

** Kensei TOBINAI, M.D., Ph.D.：国立がんセンター中央病院特殊病棟部〔〒104-0045 東京都中央区築地5-1-1〕；Hematology and Stem Cell Transplantation Division, National Cancer Center Hospital, Tokyo 104-0045, JAPAN

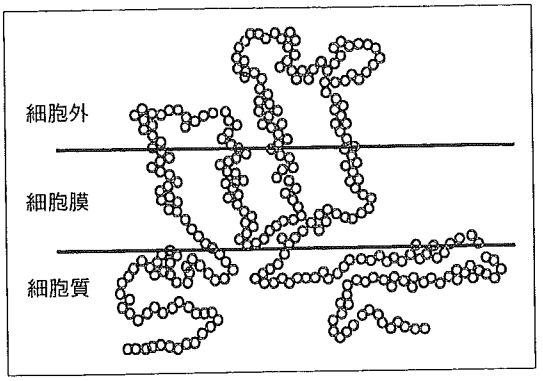

図1　CD20抗原の模式図

or cross fire effect)が期待できる．

B細胞リンパ腫に対するradioimmunotherapyに用いられる放射性同位元素の中でもっとも精力的に検討されてきたのは^{131}Iと^{90}Yである．表1に^{131}Iと^{90}Yの主な特徴を比較して示す．Radioimmunotherapyの抗腫瘍効果の主体となっているのはβ線であり，^{131}Iに比べ^{90}Yはβ線としてのエネルギー量が大きく，飛程距離(path length)が長いことより殺細胞効果が高いことが期待される．遊離した放射性同位元素の主な分布臓器は，^{131}Iが甲状腺と胃であるのに対し^{90}Yは骨である．^{90}Y標識抗体に比べ^{131}I標識抗体は体外排出量が多い．^{131}Iがβ線とγ線を放出するのに対し，^{90}Yはβ線のみを放出するため，画像診断ができない欠点があるもののradiation exposureの点で有利である．

表2に，B細胞リンパ腫に対して臨床的検討が活発に行われてきた2種類の抗CD20 radioimmunoconjugateであるibritumomab tiuxetan (Zevalin®)とtositumomab(Bexxar®)の主な特徴を比較して示す．

B細胞リンパ腫に対する通常量の抗CD20 radioimmunoconjugatesの臨床試験

1．^{131}I標識マウス型抗CD20抗体(^{131}I-tositumomab，^{131}I-Bexxar®)

Tositumomabはヒト CD20抗原に対するマウス型mAbであり，tositumomabに^{131}Iを標識したradioimmunoconjugateが^{131}I-tositumomabである．Preclearing unlabeled antibody(cold antibody)としてはマウス型抗CD20抗体tositumomab(anti-B1)が用いられる．

表1　Yttrium-90とiodine-131の主な性質の比較

Properties	Yttrium-90	Iodine-131
Energy	β emitter (2.3 MeV)	γ(0.36MeV)/ β(0.6MeV) emitter
Path length	5 mm	1 mm for β component
Administration	outpatient	inpatient or outpatient with restrictions
Half-life	64 hours	192 hours

(1) Michigan大学単施設における臨床試験

化学療法後に再発・再燃したB細胞リンパ腫59例に対し，自家造血幹細胞移植(autologous hematopoietic stem cell transplantation；AHSCT)施行例，未施行例の2つのcohortに対して1回投与でdose-escalation studyが行われ，total-body radiation dose(TBD)としての最大耐量(maximum tolerated dose；MTD)は，AHSCT施行例で45cGy，未施行例で75cGyであった．59例中42例(71%)が奏効した．低悪性度B細胞リンパ腫もしくは組織学的進展を示した42例の奏効割合83%(35/42)に対し，中悪性度B細胞リンパ腫の奏効割合は41%(7/17)であった．奏効42例の無増悪生存期間(progression-free survival；PFS)の中央値は12か月であり，7例は完全奏効(complete response；CR)を3～5.7年間維持した．原病増悪後に^{131}I-tositumomabの再投与を受けた16例中9例が再び奏効し，うち5例がCRに達した．用量制限毒性(dose-limiting toxicity；DLT)は血液毒性であり，HAMAが10例(17%)に検出された．長期観察の結果，5例に甲状腺刺激ホルモン(TSH)上昇が，骨髄異形成症候群(myelodysplastic syndrome；MDS)合併が5例に，固形がん合併が3例に認められた[3]．

(2) 再発・再燃B細胞リンパ腫に対する多施設共同第Ⅱ相試験[4]

Preclearing antibodyとしての非抱合型抗CD20抗体(anti-B1)450mg前投与後に35mg(5 mCi)の^{131}I-tositumomabが投与され，患者個々の必要治療量算出のためのdosimetric studyが施行された．その7～14日後にTBDとして75cGyの^{131}I-tositumomab(血小板数10万～15万/μlの患者では

表2 代表的な2種類の抗CD20 radioimmunoconjugates

	Ibritumomab tiuxetan (Zevalin®)	Tositumomab (Bexxar®)
Preclearing unlabeled antibody:	Rituximab, chimeric Ab	Tositumomab (Anti-B1), mouse IgG2a
Radiolabeled antibody:	Ibritumomab (mouse)	Tositumomab (mouse)
Radiolabel for dosimetry:	In-111	I-131
Radiolabel for therapy:	Y-90	I-131

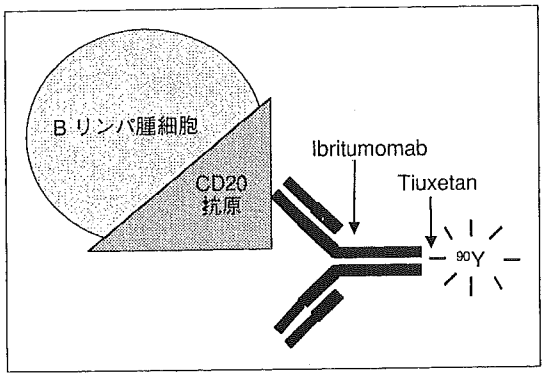

図2 ^{90}Y標識抗CD20 radioimmunoconjugateである ibritumomab tiuxetan(^{90}Y-Zevalin®)の模式図

65cGy)が投与された．47例中27例(57%)が奏効し，うち15例(32%)がCRに達した．低悪性度B細胞リンパ腫の奏効割合は57%(21/37)，中高悪性度B細胞リンパ腫への組織学的進展例の奏効割合は60%(6/10)であった．主な薬物有害反応(adverse drug reaction；ADR)は血液毒性で，倦怠感，悪心・嘔吐，発熱，感染症，瘙痒感，発疹などの非血液毒性は軽度もしくは中等度でありHAMA検出は1例のみであった[4]．

(3)化学療法抵抗性B細胞リンパ腫に対する多施設共同第II相試験[5]

2レジメン以上の化学療法治療歴があり，直前の化学療法が奏効しない，もしくは6か月以内に増悪を示した60例(低悪性度B細胞リンパ腫36例，組織学的進展23例，マントル細胞リンパ腫1例)に対し施行された．直前化学療法の奏効割合28%に比べ，^{131}I-tositumomabの奏効割合は65%(39/60)と高く($p<0.001$)，CRが12例(20%)に得られた．奏効持続期間中央値は6.5か月で，直前化学療法(3.4か月)より長かった($p<0.001$)．HAMAが5例(8%)に，TSH上昇が1例(2%)に，MDS発症が4例に認められた．

2. ^{90}Y標識マウス型抗CD20抗体(ibritumomab tiuxetan，^{90}Y-Zevalin®)

Ibritumomabはrituximab作製に用いられたマウス型抗CD20抗体であり，^{90}Yがtiuxetan(MX-DTPA)というlinker chelatorによってibritumomabに標識されている(図2)．^{90}Yはβ線のみを放出するため，画像診断やdosimetry studyにはγ線を放出する^{111}Inを標識した^{111}In-ibritumomab tiuxetanが用いられ，治療薬としては^{90}Yを標識した^{90}Y-ibritumomab tiuxetanが用いられる．

再発・再燃B細胞リンパ腫に対する第I/II相試験[6]の結果に基づき，day 1のpreclearing unlabeled antibodyとしてのrituximab投与後に^{111}In-ibritumomab tiuxetanが投与され，day 8のrituximab投与後に0.4mCi/kgの^{90}Y-ibritumomab tiuxetanが投与される．対象は骨髄中リンパ腫細胞25%未満，血小板数15万/μl以上の患者に限定され，血小板数10万～15万/μlの患者では^{90}Y-ibritumomab tiuxetanの投与量が0.3mCi/kgに減量されている．図3にibritumomab tiuxetanの投与スケジュールを示す[7]．

(1)Stanford大学単施設での第I/II相試験[8]

^{111}In標識抗CD20抗体の体内分布に基づく非標識抗CD20抗体前投与の妥当性，AHSCT非併用での^{90}Y標識抗CD20抗体のMTD，および再発・再燃B細胞リンパ腫患者に対する安全性と有効性の検討を目的に，1回投与でdose-escalation studyが施行された．Preclearing antibodyとしての非標識抗CD20抗体の前投与により^{90}Y標識抗CD20抗体の腫瘍病変への集積率が高まることが確認された．非血液毒性は軽度でありDLTは血液毒性であった．18例中6例のCRと7例の部分奏効(partial response；PR)が得られ，奏効割合は72%(13/18)であった．40mCi以下の^{90}Y標識抗CD20抗体の投与にはAHSCTによるrescueを必要としなかった．

(2)多施設共同によるphase I/II study[6]

化学療法後に再発・再燃したB細胞リンパ腫

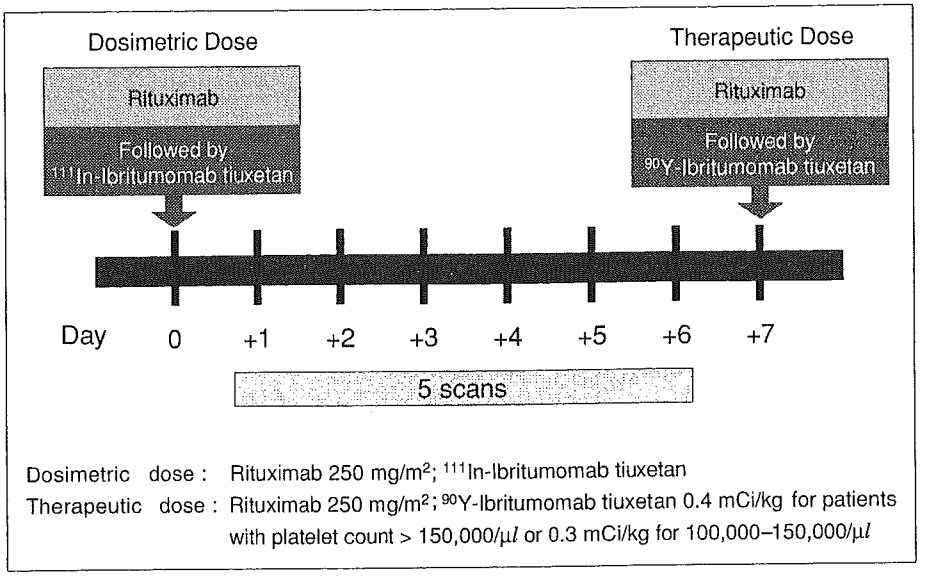

図3　Ibritumomab tiuxetan(Zevalin®)の投与スケジュール（文献[7]より引用）

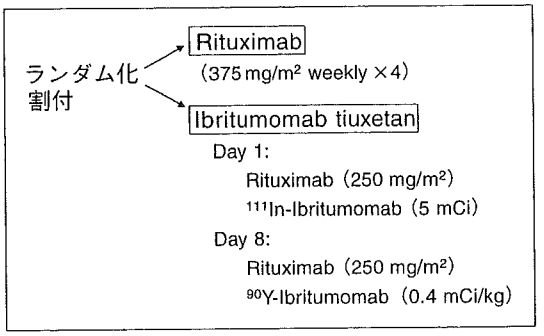

図4　Ibritumomab tiuxetanとrituximabの比較試験のデザイン（文献[11]より引用）

患者を対象に，day 1とday 8にrituximabが前投与され，1回投与でdose-escalation studyが施行された．^{90}Y-ibritumomab tiuxetanのDLTは血液毒性であり，治療開始前の骨髄中リンパ腫細胞浸潤の程度と治療前血小板数が血液毒性発現に相関し，HAMAが検出されたのは1例のみであった．血小板数15万/μl以上での^{90}Y-ibritumomab tiuxetanのMTDは0.4mCi/kgであり，血小板数10万～15万/μlでは0.3mCi/kgであった．適格51例中13例のCRと21例のPRが得られ，奏効割合は67％(34/51)であった．低悪性度B細胞リンパ腫の奏効割合は82％(28/34)で，中悪性度B細胞リンパ腫では43％(6/14)であった．奏効例の増悪までの期間time to progression(TTP)中央値は12.9か月以上であった．

(3) Rituximab不応の濾胞性リンパ腫に対する第Ⅱ相試験[9]

化学療法後に再発・再燃した濾胞性リンパ腫54例に対して施行された．一過性のgrade 4の好中球減少を35％に，grade 4の血小板減少を9％に認め，入院治療を要する感染症合併を7％に認めた．国際ワークショップ規準[10]による奏効割合は74％で，完全奏効割合(％CR)は15％であった．

(4) 化学療法後に再発・再燃した低悪性度B細胞リンパ腫に対するrituximabとの比較試験[11]

低悪性度B細胞リンパ腫，濾胞性リンパ腫もしくは組織学的進展の計143例を対象に施行された．図4に本比較試験のデザインを示す．Rituximabは375mg/m^{2}で週1回，4回投与された．Ibritumomab tiuxetan群に認められた主な毒性は血液毒性であるが，いずれも一過性であった．Ibritumomab tiuxetan群の32％にgrade 4の好中球減少を，5％にgrade 4の血小板減少を認めた．放射線診断医による独立した効果判定委員会が国際ワークショップ規準に従って判定した奏効の結果を表3に示す．奏効割合はibritumomab tiuxetan群80％，rituximab群56％(p=0.002)で，CR到達例の割合はibritumomab tiuxetan群30％，

表3 再発・再燃低悪性度B細胞リンパ腫に対するibritumomab tiuxetanとrituximabの比較試験における両群の有効性

Response	Ibritumomab tiuxetan		Rituximab		*p*-value
	n=73	95% CI	n=70	95% CI	
ORR	80%	68～88	56%	43～67	0.002
CR	30%		16%		0.040
CRu	4%		4%		
PR	45%		36%		

CI：confidence interval, ORR：overall response rate, CR：complete response, CRu：complete response unconfirmed, PR：partial response（文献[11]より引用）

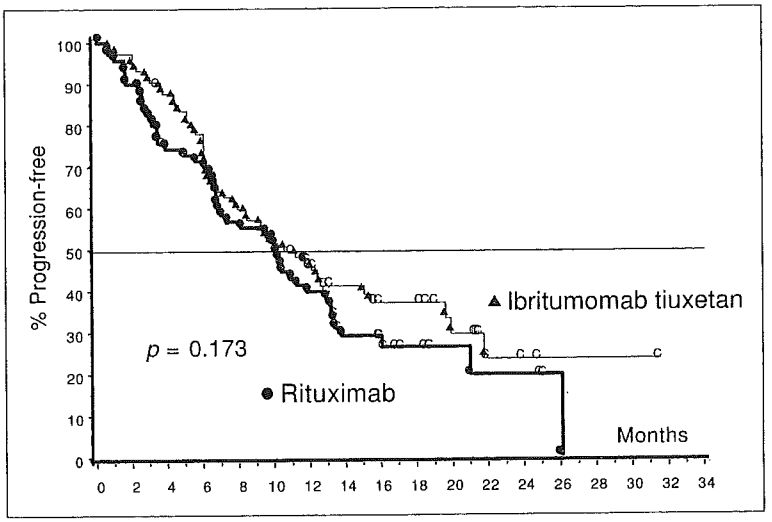

図5 Ibritumomab tiuxetanとrituximabの比較試験における両群のtime to progression（文献[11]より引用）

rituximab群16%（p=0.04）であった．奏効例に限定した奏効持続期間（duration of response）中央値はibritumomab tiuxetan群で14.2か月，rituximab群で12.1か月（p=0.6）であり，登録全例のTTP中央値はibritumomab tiuxetan群で11.2か月，rituximab群で10.1か月（p=0.173）であった（図5）．Ibritumomab tiuxetan投与後に再発・再燃して後治療が施行されるまでの期間の中央値はibritumomab tiuxetan群で11.5か月，rituximab群で7.8か月であった．再発・再燃B細胞リンパ腫に対して，ibritumomab tiuxetanは安全かつ有効な治療手段であり，その有効性はrituximabを上回ると結論された．

(5) 血小板数10万～15万/μlの患者におけるibritumomab tiuxetanの多施設共同第II相試験[12]

化学療法後に再発・再燃した低悪性度B細胞リンパ腫30例を対象に，0.3mCi/kg（11MBq/kg）〔最大投与量32mCi（1.2GBq）〕の^{90}Y-ibritumomab tiuxetanが投与された．登録された30例の年齢中央値は61歳，登録時の臨床病期は90%がIII/IV期，83%が濾胞性リンパ腫で67%が骨髄浸潤を伴っており，前治療レジメン数の中央値は2であった．正常臓器の推定吸収線量は全例において最大許容値以下であった．国際ワークショップ規準による奏効割合は83%で，CR到達例は37%であり，登録全30例のTTP中央値は9.4か月であった．主なADRは血液毒性であり，grade 4の好中球減少と血小板減少の頻度は，それぞれ33%と13%であった．軽度血小板減少例に対する減量した^{90}Y-ibritumomab tiuxetanの投与は安全かつ有効と結論された．

(6) Ibritumomab tiuxetanのdosimetry studyと安全性に関するさらなる検討

図6に，4つの臨床試験においてibritumomab

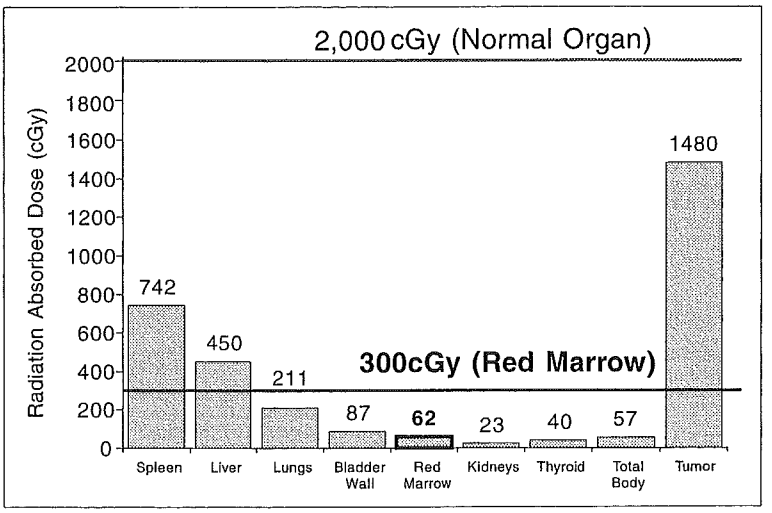

図6　Ibritumomab tiuxetanを投与された再発・再燃B細胞リンパ腫179例における各臓器の吸収線量中央値
2,000cGyはすべての正常臓器許容吸収線量上限値，300cGyは赤色骨髄の上限値．
（文献[13]より引用）

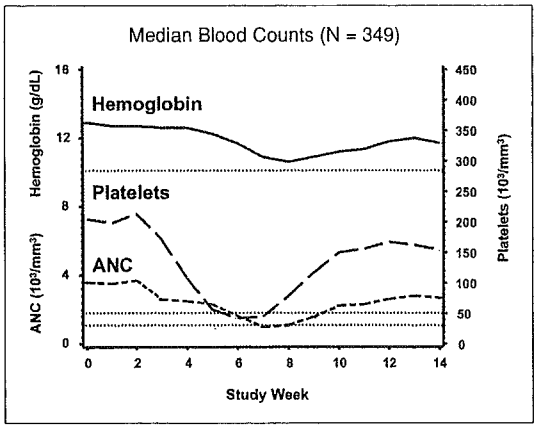

図7　Ibritumomab tiuxetanを投与された349例における血球数中央値の推移　（文献[14]より引用）

tiuxetanを投与された再発・再燃B細胞リンパ腫179例に対するdosimetry studyによって得られた各正常臓器の吸収線量の中央値を示す[13]．Ibritumomab tiuxetanの臨床試験においては正常臓器の許容吸収線量上限値が2,000cGyに，赤色骨髄の許容吸収線量上限値が300cGyに設定されていたが，これらの上限値を上回って異常な正常臓器への分布を示した例は認められなかった．このdosimetry studyではibritumomab tiuxetanの主な毒性である血液毒性と赤色骨髄の吸収線量，TBD，薬物動態学的parameter（blood effective half life, blood area under the curve［AUC］, etc.）との関連が検討されたが，明らかな相関は認められなかった．

図7に，^{90}Y-ibritumomab tiuxetanを投与された349例の血球数の中央値の推移を示す[14][15]．^{90}Y-ibritumomab tiuxetan投与後の好中球減少と血小板減少は通常の抗がん剤治療より緩徐に出現して5～7週後に最低値を示すが，好中球数の最低値出現時期は血小板最低値出現時期よりわずかに遅れる傾向がある．0.4mCi/kg投与例におけるgrade 4の好中球減少と血小板減少の発現頻度はそれぞれ30％と10％であり，0.3mCi/kg投与例における発現頻度（35％と14％）の方がわずかに高い．すなわち，治療開始前の血小板数10万～15万/μlの例では^{90}Y-ibritumomab tiuxetanを3/4に減量してもより重度の血球減少を発現する可能性を考慮する必要性がある．血液毒性発現の程度と治療開始前の骨髄浸潤の程度は相関した．感染症合併のために入院治療を必要とした患者は7％で，grade 3以上の出血は2％の患者に認められた．治療終了8～34か月後に，5例（1％）がMDSもしくは急性骨髄性白血病を発症した．骨髄中のリンパ腫細胞が25％未満で，血小板数10万/μl以上，好中球数1,500/μl以上と十分な骨髄機能が保持されている再発・再燃B細胞リン

パ腫患者において^{90}Y-ibritumomab tiuxetanの1回投与は十分に安全であると結論された[14]．Ibritumomab tiuxetan治療に伴う輸注関連毒性の大半はgrade 1もしくはgrade 2であり，rituximab投与によるADRと考えられた．

Radioimmunotherapyでは治療関連MDS/白血病の発生が増える可能性が懸念されていた．4つの臨床試験に登録されてibritumomab tiuxetanを投与された211例の観察結果が2004年の米国臨床腫瘍学会(American Society of Clinical Oncology；ASCO)に報告された[16]．対象患者の前治療レジメン数の中央値は2(1～9)であった．Ibritumomab tiuxetan投与後の観察期間中央値38か月(1.2～75.5か月)時点の解析で7例(3.3%)が治療関連MDS/白血病を発症していた．治療関連MDS/白血病を発症した7例におけるibritumomab tiuxetan投与後から治療関連白血病発症までの期間の中央値は18か月(8～50か月)で，リンパ腫の診断から白血病発症までの期間の中央値は8年(4.3～14年)であった．リンパ腫患者における治療開始後2～10年における治療関連白血病の発症リスクは1～1.5%/年とされていることを考慮すると，ibritumomab tiuxetan投与例における治療関連白血病の発生頻度は対照群に比べ高くないことが示唆される．大半の治療関連白血病患者において5番および7番染色体の異常が検出されており，アルキル化剤を主体とした前治療との関連が示唆される．上記4つの臨床試験以外の設定でibritumomab tiuxetanを投与された535例の観察期間中(0～36.5か月)に5例の治療関連白血病の発生が認められたが，うち2例はibritumomab tiuxetan投与前の骨髄染色体検査に異常が認められていた．Ibritumomab tiuxetan投与例におけるこれまでの観察結果をみるかぎり，治療関連白血病の年間発生頻度は厳しい前治療歴を有する今回の検討対象に予期される発生頻度に合致するものであり，ibritumomab tiuxetanによるradioimmunotherapyによって治療関連白血病の発生頻度は増加しないことが示唆される[16]．

Radioimmunotherapyでは遅発性の骨髄抑制がDLTとなるため，radioimmunotherapy施行後に十分量の化学療法施行が可能か否かが懸念される．5つの臨床試験において0.4mCi/kgの^{90}Y-ibritumomab tiuxetanを投与された58例に関する単施設の検討結果がMayo Clinicより報告された[17]．58例全例が，ibritumomab tiuxetan投与後に原病増悪を認めたために後治療を受けていた．同時期に同施設においてibritumomab tiuxetan以外の治療を受けた患者を対照として比較検討が行われた．Ibritumomab tiuxetan投与後の後治療のレジメン数中央値は2(1～7)であった．17例(28%)が造血サイトカインを投与されたが，血球減少遷延のために化学療法剤の減量を余儀なくされたのは2例に過ぎなかった．8例ではibritumomab tiuxetan投与後に採取された造血幹細胞を用いて自家造血幹細胞移植が施行された．Ibritumomab tiuxetan以外の治療を受けた対照群に比べ毒性発現の程度には差を認めなかった．Ibritumomab tiuxetan投与後においても化学療法や自家造血幹細胞移植は施行可能であることが結論された．

AHSCTを併用したradioimmunotherapy

RadioimmunoconjugateのDLTは血液毒性であるため，AHSCT併用により増量が可能である．B細胞リンパ腫を対象に，AHSCTを併用して^{131}I標識抗CD20抗体を大量投与する治療研究がPressらによって施行されている[18]．正常臓器の最大許容線量は27Gyであり，AHSCT併用でのDLTは心肺毒性であった．29例中25例(86%)が奏効し，23例(79%)がCRに達し，11例(39%)が後治療なしで5年以上無病生存している．

わが国でのibritumomab tiuxetanの臨床開発

米国に比べわが国ではradioimmunotherapyへの取組みが遅れていたが，核医学の専門家の全面的な協力の下に，2002年よりibritumomab tiuxetanの第Ⅰ相試験が国立がんセンター中央病院と東病院の2施設で施行され，その研究結果が2004年の日本癌学会に報告された[19]．化学療法後に再発・再燃した低悪性度B細胞リンパ腫患者に対するibritumomab tiuxetanによるradioimmunotherapyの安全性と薬物動態，dosimetry，有効性の検討を目的として施行された．Day 1に^{111}In-ibritumomab tiuxetanを3.5～5.0mCi投与し，γカメラ撮像

での^{111}In-ibritumomab tiuxetanの分布像より^{90}Y-ibritumomab tiuxetanの投与の可否を判断し，day 8に^{90}Y-ibritumomab tiuxetanを0.3mCi/kgと0.4mCi/kgの2用量で投与した．増量可否の判断根拠となる臨界毒性を，3週間以上持続する25,000/μl未満の血小板減少，3週間以上持続するgrade 4の好中球減少と，grade 3以上の非血液毒性と規定した．化学療法施行後に再発・再燃した濾胞性リンパ腫9例とマントル細胞リンパ腫1例の計10例に^{90}Y-ibritumomab tiuxetanを投与した．臨界毒性発現は0.3mCi/kg群で3例中0例(1例は原病増悪で死亡)，0.4mCi/kg群で6例中2例(低Na血症など1例，好中球減少・血小板減少など1例)で，^{90}Y-ibritumomab tiuxetanのrecommended phase Ⅱ doseを0.4mCi/kgと判断した．好中球減少の発現はgrade 3が4例，grade 4が3例で，血小板減少発現はgrade 3が3例であった．薬物動態学的検討結果とdosimetry studyの結果は先行して実施された米国臨床試験の結果と類似した．10例中5例がCR，2例がPRに達し，奏効割合は70%(7/10)であった．Ibritumomab tiuxetanの再発・再燃低悪性度B細胞リンパ腫に対する安全性と高い有効性を確認できた．現在，わが国初のradioimmunotherapyの承認取得を目指して，参加施設を拡大して第Ⅱ相試験を実施中である．

おわりに

mAbによる悪性腫瘍の治療研究は，多くの障害を乗り越えて臨床的有用性が確立された．なかでも，B細胞リンパ腫に対するキメラ型抗CD20抗体rituximabと抗CD20 radioimmunoconjugateの研究が精力的に進められている．Radioimmunoconjugateは非抱合型抗体を上回る抗腫瘍効果を有し，今後の発展が大いに期待される分野である．2002年に米国食品医薬品庁(FDA)によって^{90}Y-ibritumomab tiuxetan(^{90}Y-Zevalin®)が承認され，^{131}I-tositumomab(^{131}I-Bexxar®)も2003年に承認された．わが国においても^{90}Y-ibritumomab tiuxetanの開発治験が進行しており，今後，わが国のB細胞リンパ腫治療においてもradioimmunotherapyが重要な役割を発揮することが期待される．

文　献

1) Reff ME, Carner K, Chambers KS, et al. Depletion of B cells in vivo by a chimeric mouse human monoclonal antibody to CD20. Blood 1994 ; 83 : 435.
2) Tobinai K. Monoclonal antibody therapy for B-cell lymphoma : clinical trials of an anti-CD20 monoclonal antibody for B-cell lymphoma in Japan. Int J Hematol 2002 ; 76 : 411.
3) Kaminski MS, Estes J, Zasadny KR, et al. Radioimmunotherapy with iodine(131)I tositumomab for relapsed or refractory B-cell non-Hodgkin lymphoma : updated results and long-term follow-up of the University of Michigan experience. Blood 2000 ; 96 : 1259.
4) Vose JM, Wahl RL, Saleh M, et al. Multicenter phase Ⅱ study of iodine-131 tositumomab for chemotherapy-relapsed/refractory low-grade and transformed low-grade B-cell non-Hodgkin's lymphomas. J Clin Oncol 2000 ; 18 : 1316.
5) Kaminski MS, Zelenetz AD, Press OW, et al. Pivotal study of iodine I 131 tositumomab for chemotherapy-refractory low-grade or transformed low-grade B-cell non-Hodgkin's lymphomas. J Clin Oncol 2001 ; 19 : 3918.
6) Witzig TE, Whiter CA, Wiseman GA, et al. Phase I/Ⅱ trial of IDEC-Y2B8 radioimmunotherapy for treatment of relapsed or refractory CD20$^+$ B-cell non-Hodgkin's lymphoma. J Clin Oncol 1999 ; 17 : 3793.
7) Wiseman GA, White CA, Stabin M, et al. Phase I/Ⅱ ^{90}Y-Zevalin (yttrium-90 ibritumomab tiuxetan, IDEC-Y2B8) radioimmunotherapy dosimetry results in relapsed or refractory non-Hodgkin's lymphoma. Eur J Nucl Med 2000 ; 27 : 766.
8) Knox SJ, Goris ML, Trisler K, et al. Yttrium-90-labeled anti-CD20 monoclonal antibody therapy of recurrent B-cell lymphoma. Clin Cancer Res 1996 ; 2 : 457.
9) Witzig TE, Flinn IW, Gordon LI, et al. Treatment with ibritumomab tiuxetan radioimmunotherapy in patients with rituximab-refractory follicular non-Hodgkin's lymphoma. J Clin Oncol 2002 ; 20 : 3262.

10) Cheson BD, Horning SJ, Coiffier B, et al. Report of an international workshop to standardize response criteria for non-Hodgkin's lymphomas. J Clin Oncol 1999 ; 17 : 1244.
11) Witzig TE, Gordon LI, Cabanillas F, et al. Randomized controlled trial of yttrium-90-labeled ibritumomab tiuxetan radioimmunotherapy versus rituximab immunotherapy for patients with relapsed or refractory low-grade, follicular, or transformed B-cell non-Hodgkin's lymphoma. J Clin Oncol 2002 ; 20 : 2453.
12) Wiseman GA, Gordon LI, Multani PS, et al. Ibritumomab tiuxetan radioimmunotherapy for patients with relapsed or refractory non-Hodgkin lymphoma and mild thrombocytopenia : a phase II multicenter trial. Blood 2002 ; 99 : 4336.
13) Wiseman GA, Kornmehl E, Leigh B, et al. Radiation dosimetry results and safety correlations from ^{90}Y-ibritumomab tiuxetan radioimmunotherapy for relapsed or refractory non-Hodgkin's lymphoma : combined data from 4 clinical trials. J Nucl Med 2003 ; 44 : 465.
14) Witzig TE, White CA, Gordon LI, et al. Safety of yttrium-90 ibritumomab tiuxetan radioimmunotherapy for relapsed low-grade, follicular, or transformed non-Hodgkin's lymphoma. J Clin Oncol 2003 ; 21 : 1263.
15) Emmanouilides CE, Witzig TE, Molina A, et al. Improved safety and efficacy of yttrium-90 ibritumomab tiuxetan radioimmunotherapy when administered as 2nd or 3rd line therapy for relapsed low-grade, follicular, and transformed B-cell non-Hodgkin's lymphoma. Proc Am Soc Clin Oncol 2003 ; 22 : 595 (abstr 2392).
16) Emmanouilides C, Czuczman MS, Revell S, et al. Low incidence of treatment-related myelodysplastic syndrome and acute myelogenous leukemia in patients with non-Hodgkin's lymphoma treated with ibritumomab tiuxetan. Proc Am Soc Clin Oncol 2004 ; 22 : abstr 6696.
17) Ansell SM, Ristow KM, Habermann TM, et al. Subsequent chemotherapy regimens are well tolerated after radioimmunotherapy with yttrium-90 ibritumomab tiuxetan for non-Hodgkin's lymphoma. J Clin Oncol 2002 ; 20 : 3885.
18) Liu SY, Eary JF, Petersdorf SH, et al. Follow-up of relapsed B-cell lymphoma patients treated with iodine-131-labeled anti-CD20 antibody and autologous stem-cell rescue. J Clin Oncol 1998 ; 16 : 3270.
19) 伊藤國明，渡辺　隆，五十嵐忠彦，ほか．Indolent B 細胞性リンパ腫に対する免疫放射線療法^{90}Y-ibritumomab tiuxetanの第Ⅰ相試験．日本癌学会学術総会記事 2004 ; 357, P-1039.

*　　*　　*

International Journal of
HEMATOLOGY

Letter to the Editor

A Case of Interstitial Pneumonia Induced by Rituximab Therapy

Junji Hiraga,[a] Yasuhiro Kondoh,[b] Hiroyuki Taniguchi,[b] Tomohiro Kinoshita,[a] Tomoki Naoe[a]

[a]*Department of Hematology, Nagoya University Graduate School of Medicine, Nagoya;* [b]*Department of Respiratory Medicine and Allergy, Tosei General Hospital, Seto, Japan*

Received October 26, 2004; received in revised form December 7, 2004; accepted December 8, 2004

Int J Hematol. 2005;81:169-170. doi: 10.1532/IJH97.04163

Rituximab, a chimeric human/murine monoclonal antibody directed against CD20, is an effective therapy for B-cell type non-Hodgkin's lymphoma. Most of the adverse responses are mild to moderate nonhematological toxicities, which include fever, chill, or skin reactions. Severe respiratory adverse events have been infrequent [1,2]. Recently, Burton et al reported 2 interstitial pneumonia (IP) cases related to rituximab therapy [3]. IP is rarely induced by rituximab, and its etiological roles are still unclear. Here, we report an IP case related to rituximab therapy, for which we investigated its etiology as well as possible.

An 80-year-old man with a diagnosis of diffuse large B-cell lymphoma was treated with rituximab and cyclophosphamide, vincristine, and prednisolone chemotherapy (R-COP). No severe adverse effects were observed during the first course, and after 3 weeks, he was given a second course. With the second rituximab infusion, he had a grade 2 fever and a systemic skin rash. The infusion reaction was abated with hydroxycortisone, and COP therapy was scheduled. Ten days after the second rituximab infusion, the patient complained of general fatigue and had a high fever. A chest x-ray revealed bilateral ground-glass opacities, and a high-resolution computed tomography scan of the chest confirmed the diagnosis of interstitial pneumonia. As respiratory insufficiency advanced, he needed noninvasive positive-pressure ventilation. He was treated with methylprednisolone pulse therapy after a bronchoalveolar lavage (BAL) examination. He made a dramatic recovery, corticosteroid was tapered, and he was discharged after 3 weeks.

No pathogens were detected in the patient's blood, sputum, or BAL fluids, and results for *Pneumocystis carini* and *Mycobacterium tuberculosis* were also negative. Serum antibodies did not indicate the presence of viruses, chlamydia pneumonia, legionella, or mycoplasma pneumonia. Lymphocytes were 40.4% and $CD4^+$ T-cells comprised 86% of the lymphocyte in the BAL fluids. Antineutrophil cytoplasmic factors, rheumatoid factors, and antinuclear antibodies were not detected. A cytological examination showed no malignant cells in the BAL fluids.

Human antichimeric antibodies (HACA) were reported as a cause of acute lung injury in a patient with Crohn's disease who was treated with Infliximab [4]. We examined our patient's plasma, which was obtained 2 months after his rituximab treatment, for HACA and to determine the rituximab level. Both HACA and rituximab were undetectable. A drug lymphocyte stimulation test (DLST) was reported to be positive in a patient who was allergic to a drug that induced IP in the patient [5]. We conducted DLST for rituximab, cyclophosphamide, and vincristine in our patient and found that only rituximab showed as strongly positive. Tumor necrosis factor α, interferon γ, and interleukin 4 were elevated in his serum level, findings that proved to be similar to the previous report of rituximab-induced IP [3]. Klebsvonden Lungen-6 (KL-6) is also known as a marker of drug-induced IP, especially of the diffuse-alveolar type [6]. In our case, KL-6 was within the normal range.

These results strongly suggested that in this patient, IP was induced by rituximab and that the T-cells activated by rituximab took part in IP development. Further evaluation of T-cell immunity related to rituximab will clarify IP mechanisms in patients treated with rituximab.

References

1. McLaughlin P, Grillo-Lopez AJ, Link BK, et al. Rituximab chimeric anti-CD20 monoclonal antibody therapy for relapsed indolent lymphoma: half of patients respond to a four-dose treatment program. *J Clin Oncol.* 1998;16:2825-33.
2. Tobinai K. Monoclonal antibody therapy for B-cell lymphoma: clinical trials of an anti-CD20 monoclonal antibody for B-cell lymphoma in Japan. *Int J Hematol.* 2002;76:411-419.
3. Burton C, Kaczmarski R, Jan-Mohamed R. Interstitial pneumonitis related to rituximab therapy. *N Engl J Med.* 2003;348:2690-2691.

Correspondence and reprint requests: Junji Hiraga, MD, Department of Hematology, Nagoya University Graduate School of Medicine, 65 Tsurumai-cho, Showa-ku, Nagoya 466-8550, Japan; 81-52-744-2145; fax: 81-52-744-2157 (e-mail: hiraga@med.nagoya-u.ac.jp).

4. Riegert-Johnson DL, Godfrey JA, Myers JL, et al. Delayed hypersensitivity reaction and acute respiratory distress syndrome following infliximab infusion. *Inflamm Bowel Dis.* 2002;8:186-191.
5. Kurakawa E, Kasuga I, Ishizuka S, et al. Interstitial pneumonia possibly due to a novel anticancer drug, TS-1: first case report. *Jpn J Clin Oncol.* 2001;31:284-286.
6. Onishi H, Yokoyama A, Yasuhara Y, et al. Circulating KL-6 levels in patients with drug induced pneumonitis. *Thorax.* 2003;58:872-875.

Enhanced Natural Killer Cell Binding and Activation by Low-Fucose IgG1 Antibody Results in Potent Antibody-Dependent Cellular Cytotoxicity Induction at Lower Antigen Density

Rinpei Niwa,[1] Mikiko Sakurada,[1] Yukari Kobayashi,[1] Aya Uehara,[1] Kouji Matsushima,[2] Ryuzo Ueda,[3] Kazuyasu Nakamura,[1] and Kenya Shitara[1]

[1]Tokyo Research Laboratories, Kyowa Hakko Kogyo, Co., Ltd.; [2]Department of Molecular Preventive Medicine, School of Medicine, University of Tokyo, Tokyo, Japan; and [3]Department of Internal Medicine and Molecular Science, Nagoya City University Graduate School of Medical Science, Nagoya, Japan

ABSTRACT

Purpose: **Recent studies have revealed that fucose removal from the oligosaccharides of human IgG1 antibodies results in a significant enhancement of antibody-dependent cellular cytotoxicity (ADCC) via improved IgG1 binding to FcγRIIIa. In this report, we investigated the relationship between enhanced ADCC and antigen density on target cells using IgG1 antibodies with reduced fucose.**

Experimental Design: **Using EL4 cell-derived transfectants with differential expression levels of exogenous human CC chemokine receptor 4 or human CD20 as target cells, ADCC of fucose variants of chimeric IgG1 antibodies specific for these antigens were measured. We further investigated IgG1 binding to natural killer (NK) cells and NK cell activation during ADCC induction to elucidate the mechanism by which low-fucose IgG1 induces ADCC upon target cells with low antigen expression.**

Results: **Low-fucose IgG1s showed potent ADCC at low antigen densities at which their corresponding high-fucose counterparts could not induce measurable ADCC. The quantitative analysis revealed that fucose depletion could reduce the antigen amount on target cells required for constant degrees of ADCC induction by 10-fold for CC chemokine receptor 4 and 3-fold for CD20. IgG1 binding to NK cells was increased by ligating IgG1 with clustered antigen, especially for low-fucose IgG1. Up-regulation of an activation marker, CD69, on NK cells, particularly the $CD56^{dim}$ subset, in the presence of both the antibody and target cells was much greater for the low-fucose antibodies.**

Conclusions: **Our data showed that fucose removal from IgG1 could reduce the antigen amount required for ADCC induction via efficient recruitment and activation of NK cells.**

INTRODUCTION

Antibodies of the human IgG1 isotype are commonly used for therapeutic applications as they can mediate multiple effector functions including antibody-dependent cellular cytotoxicity (ADCC), complement-dependent cytotoxicity (CDC), and direct apoptosis induction (1–3). ADCC, a lytic attack on antibody-targeted cells, is triggered following binding of leukocyte receptors (FcγR) to the antibody Fc region. Several mouse and clinical studies indicate that ADCC is an important therapeutic mechanism of clinically effective antibodies (4–7). FcγRIIIa is the predominant FcγR of natural killer (NK) cells responsible for ADCC activation. The FcγRIIIa gene (*FCGR3A*) displays an allelic polymorphism that generates receptors containing either a phenylalanine (F) or a valine (V) at a position critical in mediating ADCC, amino acid position 158. This variation results in human IgG1 antibodies binding with higher affinity to the NK cells of homozygous *FCGR3A*-158V donors than those of homozygous *FCGR3A*-158F donors, and seems to result in more effective NK cell activation (8, 9). Importantly, several reports have recently shown that *FCGR3A* genotype influences the clinical efficacy of human IgG1-type anti-CD20 antibody rituximab (3, 10, 11) with the clinical response of patients bearing FcγRIIIa-158F being significantly inferior to the patients with the FcγRIIIa-158V receptors (5–7). These reports underscore the importance of ADCC in clinical outcomes.

ADCC activity is influenced by the structure of complex-type oligosaccharides linked to CH2 domain of the antibody Fc region. The content of galactose (12, 13), bisecting *N*-acetylglucosamine (14, 15), and fucose (16, 17) in the antibody oligosaccharide have each been reported to effect ADCC. In previous studies, we have shown that fucose is the most critical antibody oligosaccharide component and that the removal of fucose from IgG1 oligosaccharides results in a very significant enhancement of both ADCC *in vitro* (~100 fold) and antitumor activity *in vivo* (17, 18). However, many therapeutic antibodies currently approved or under clinical development are produced using Chinese hamster ovary cells that express high level of α1,6-fucosyltransferase and consequently produce low amounts antibody lacking fucose (17). Therefore, we generated a fucosyltransferase knockout Chinese hamster ovary cell line that can stably produce nonfucosylated antibodies with enhanced ADCC (19) that behaves in other respects indistinguishable from the parental line.

Although therapeutic antibodies are demonstrating increasing success in the clinic, especially in the field of cancer treatment (1, 2), the full potential may be limited by the low and

Received 11/5/04; revised 12/21/04; accepted 12/29/04.
The costs of publication of this article were defrayed in part by the payment of page charges. This article must therefore be hereby marked *advertisement* in accordance with 18 U.S.C. Section 1734 solely to indicate this fact.

Requests for reprints: Kenya Shitara, Division of Immunology, Tokyo Research Laboratories, Kyowa Hakko Kogyo, Co., Ltd., 3-6-6 Asahi-machi, Machida-shi, Tokyo 194-8533, Japan. Phone: 81-42-725-0857; Fax: 81-42-725-2689; E-mail: kshitara@kyowa.co.jp.

variable antigen expression on the target cells. This is due to three factors that can limit the efficacy of therapeutic antibodies. First, there are often individual patients or clinical subtypes of the cancer that are unresponsive to the antibody therapy due to limited or heterogeneous antigen expression (3, 20). Second, residual tumor cells after antibody therapy may be selected to express less antigen than pretreated tumor cells (21, 22), become resistant to additional treatment, and, thus, may lead to poor prognosis. Third, antigen may be thought unsuitable as antibody targets due to low antigen expression. Consequently, it is important to improve antibody efficacy for tumor cells with lower antigen expression level.

Previous studies have shown that ADCC depends on antigen expression levels on target cells (23). Hence, we asked if low-fucose IgG1 with enhanced ADCC might overcome the problem of low antigen density on target cells. In this study, we quantitatively analyzed the effect of antigen levels on the ability of low-fucose IgG1 to induce ADCC on target cells to determine the potential therapeutic advantage of low-fucose IgG1 for future clinical applications. Additionally, we focused on NK cell binding to low-fucose IgG1 and the resultant cellular activation to understand the mechanism of potent ADCC induction, especially at low antigen density.

MATERIALS AND METHODS

Blood Donors. Blood donors were randomly selected from healthy volunteers registered at Tokyo Research Laboratories, Kyowa Hakko Kogyo, Co., Ltd. All donors gave written informed consent before analyses.

Cell Lines. Mouse T-cell lymphoma cell line EL4, human B lymphoma cell line CA46, CCRF-SB (ATCC CCL-120), ST486, Raji, and Daudi were purchased from the American Type Culture Collection (Rockville, MD). A human B lymphoma cell line P32/ISH (JCRB0095) was purchased from Health Science Research Resources Bank (Osaka, Japan).

Preparation of Target Cell Lines. A human CC chemokine receptor 4 (CCR4) expression plasmid CAG-pcDNA-CCR4 bas been previously described (18). An expression plasmid encoding human CD20, designated pKANTEXCD20, was constructed by inserting *CD20* gene, cloned from a human leukocyte cDNA library (BD Biosciences Clontech, Palo Alto, CA) by PCR into mammalian cell expression vector pKANTEX93 (24). EL4 cells were transfected with CAG-pcDNA-CCR4 or pKANTEXCD20 by electroporation and grown in the presence of 0.5 mg/mL G418 sulfate to obtain G418-resistant clones. For some clones with higher CD20 expression, gene amplification in the presence of methotorexate (4-amino-10-methylpteroylglutamic acid, MTX) was done. Multiple clones with differential protein expression levels were screened by nonquantative flow cytometry as described below.

Antigen Expression Analysis by Flow Cytometry. A nonquantitative flow cytometry was done for the screening of transfected target cell clones. Biotinylated KM2760 was prepared using EZ-Link Sulfo-NHS-LC-Biotin (Pierce, Rockford, IL) as described by the manufacturer. Approximately 1×10^6 cells were stained for 1 hour on ice with 3 μg/mL of biotin-labeled KM2760 for $CCR4^+$ clones or a 10-fold dilution of FITC-conjugated anti-CD20 monoclonal antibody (Beckman Coulter, Tokyo, Japan) for $CD20^+$ clones. For CCR4-expressing clones, cells were washed and then stained with phycoerythrin-conjugated streptavidin (Becton Dickinson Japan, Tokyo, Japan) as the secondary reagent. The stained cells were analyzed on an EPICS XL-MCL flow cytometer (Beckman Coulter).

To determine the absolute number of the antibody binding sites per cell, a quantitative flow cytometry analysis (25) was done using DAKO QIFIKIT (DakoCytomation, Kyoto, Japan). Briefly, 1×10^6 cells were stained for 1 hour on ice with saturating concentration of KM2160 (60 μg/mL) for $CCR4^+$ clones or mouse anti-CD20 monoclonal antibody (clone 2H7, BD Biosciences PharMingen, San Diego, CA; 40 μg/mL) for $CD20^+$ clones. Cells were then washed and then stained with FITC-conjugated anti-mouse IgG (DakoCytomation) for 1 hour on ice. Standard beads coated with known amount of mouse IgG molecules were also stained with FITC-conjugated anti-mouse IgG. The stained samples were analyzed using a flow cytometer, and the numbers of binding sites per cell were calculated by comparing the mean fluorescent intensity value of the stained cells to a standard curve obtained by regression analysis of the mean fluorescent intensity values of standard beads.

Cytotoxicity Assay. ADCC was measured using a standard 4-hour ^{51}Cr release assay as previously described (17). CDC was measured by a nonradioactive method. Target cells (1×10^6 cells/50 μL medium), varying concentrations of antibodies (in 50 μL medium), and human complement serum (50 μL, ×2 diluted with medium; Sigma, St. Louis, MO) were distributed into 96-well flat-bottomed plates. All cells and reagents were diluted with RPMI 1640 (Life Technologies, New York, NY) containing 10% heat-inactivated fetal bovine serum. After incubation at 37°C for 2 hours, aliquots of the cell proliferation reagent WST-1 (Roche Diagnostic GmbH, Penzberg, Germany) were added to each well (15 μL) and the plates were incubated for a further 4 hours to allow the formazan dye production by the metabolically active cells. The percent cytotoxicity was calculated from the absorbance at 450 nm minus the reference absorbance at 650 nm ($A_{450} - A_{650}$) of each well according to the formula:

$$\% \text{ cytotoxicity} = 100 \times (E - S)/(M - S)$$

where E is the $A_{450} - A_{650}$ of experimental well, S is that in the absence of monoclonal antibody (cells were incubated with medium and complement alone), and M is that of medium and complement alone.

Isolation of Natural Killer Cells. Peripheral blood mononuclear cells (PBMC) were prepared from peripheral blood by density gradient centrifugation using Lymphoprep (AXIS SHIELD, Dundee, United Kingdom). PBMC were then subjected to negative magnetic sorting to obtain NK cell fraction, by removing CD3, CD14, CD19, CD36, and IgE-positive cells using MACS NK cell isolation kit and MidiMACS (Miltenyi Biotec, Bergisch Gladbach, Germany). The phenotype of the isolated NK cell fraction was confirmed as >95% $CD56^+CD3^-$ before any experiments.

IgG1 Binding Analysis to Natural Killer Cells. Isolated NK cells (1×10^6) were incubated on ice for 1 hour with 1% bovine serum albumin (BSA)/PBS containing 10 μg/mL IgG1. After incubation with IgG1, cells were washed twice with PBS

and analyzed after staining with phycoerythrin-conjugated anti-human IgG Fab'$_2$ (DakoCytomation) on a flow cytometer. In some experiments, IgG1 was incubated with 20 μg/mL BSA-conjugated CCR4 peptide before the incubation with NK cells for the IgG1 ligation. The BSA-conjugated CCR4 peptide was prepared by conjugating the partial CCR4 peptide including the binding site of KM2760 and KM3060 (corresponding to amino acid residues 2 to 29 of human CCR4; ref. 18) to the amino groups of BSA using 4-(*N*-maleimidomethyl)-cyclohexane-1-carboxylate *N*-hydroxysuccinimido ester (Sigma) as previously described (26).

Analysis of Natural Killer Cell Activation. Isolated NK cells (1×10^5/100 μL medium/well) and the equal number of target cells in 100 μL medium were dispensed in round-bottom 96-well plate. IgG1 (final concentration, 1 μg/mL) or medium alone were added to each well and incubated at 37°C. Cells were harvested periodically (4, 24, and 72 hours) and double-stained with phycoerythrin-conjugated anti-CD56 monoclonal antibody (Beckman Coulter) and FITC-conjugated anti-CD69 monoclonal antibody (BD Biosciences PharMingen) on ice for 1 hour. After washing, NK cells, which can be gated out by their relative smaller values of forward scatter and side scatter compared with target cells, were measured of their CD56/CD69 expression on a flow cytometer.

RESULTS

Antibody-Dependent Cellular Cytotoxicity of Anti-CD20 IgG1 Fucose Variants against B Lymphoma Cell Lines with Differential CD20 Expression Levels. KM3065 (17) is a low-fucose variant of anti-CD20 chimeric IgG1 rituximab, which is widely used for the treatment of B-cell disorders. KM3065 and rituximab have identical amino acid sequences and thus show identical CD20 binding activities, whereas they differ in the percentage of antibody lacking fucose-containing carbohydrates linked to Asn^{297} in CH2 domain of heavy chain (Table 1). Due to its low fucose contents and consequent strong FcγRIIIa binding, KM3065 has been shown to exhibit enhanced ADCC against CD20$^+$ Raji cells and WIL2-S cells (17, 27). However, how the ADCC enhancement by defucosylation was influenced by the intrinsic properties of target cells remains to be verified. To investigate the relationships between the enhancement of ADCC by defucosylation and the antigen expression level on target cells, we investigated ADCC of the two anti-CD20 IgG1s upon six B lymphoma cell lines with differential CD20 expression levels as shown in Fig. 1. CD20 binding sites on each cell lines were determined by quantitative flow cytometry method (25) with values ranging within an order of magnitude (7.8×10^4 to 5.9×10^5). Using human PBMCs with effector cells, KM3065

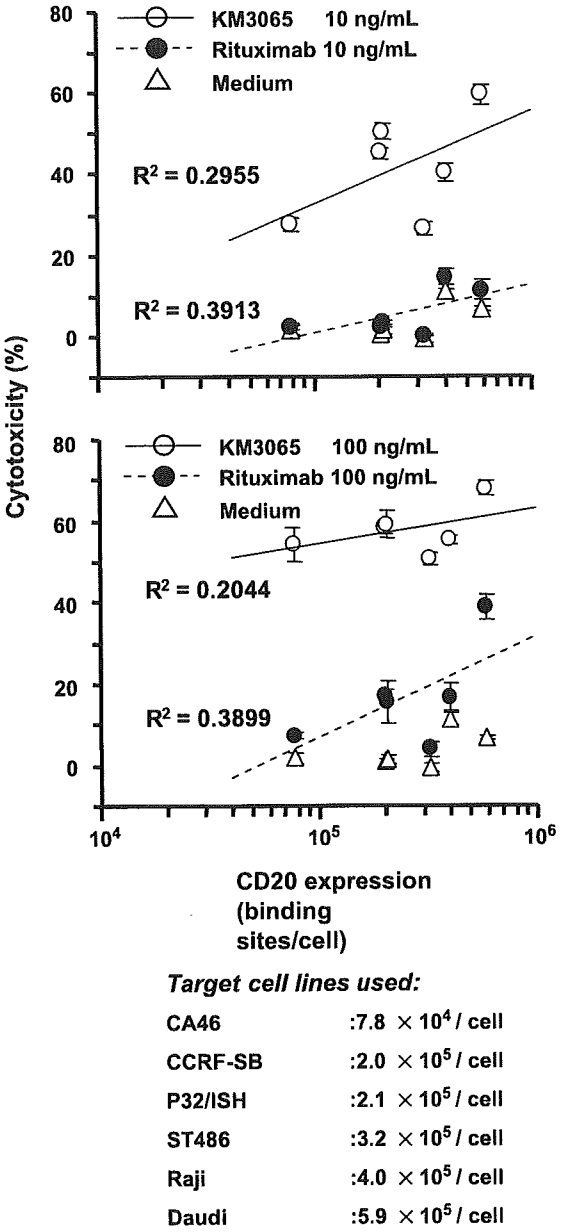

Fig. 1 ADCC of anti-CD20 chimeric IgG1s against B lymphoma cell lines with differential CD20 expression. The cytotoxicities in the presence of 10 ng/mL (*top*) or 100 ng/mL (*bottom*) of anti-CD20 IgG1s against six B lymphoma cell lines determined by 4-hour ^{51}Cr release assays are shown. PBMC from a healthy blood donor were used as effector cells, with an effector-to target ratio of 25:1. *Y*-axis, cytotoxicity (%), mean ± SD (n = 3). *X*-axis, number of CD20 binding sites per cell on each target cell line. The target cell lines used and the corresponding numbers of CD20 binding sites were also shown.

Table 1 Content of nonfucosylated N-linked oligosaccharide in each IgG1 compositions

IgG1	Specificity	%Fucose(−)	Reference
KM2760	Human CCR4	93	Niwa et al. (18)
KM3060	Human CCR4	9	Niwa et al. (18)
KM3065	Human CD20	91	Shinkawa et al. (17)
Rituximab	Human CD20	6	Shinkawa et al. (17)

showed enhanced ADCC upon all the target cell lines compared with rituximab. Although the correlation between the ADCC and the numbers of CD20 binding sites was not statistically significant, ADCC values mediated by both the two IgG1s tended to be higher for target cell lines with higher CD20 expression. The result suggests that target cell lines from different origins are not suitable for the quantitative analysis of ADCC depending on antigen expression because their own

cellular backgrounds, other than the antigen amount, determines their inherent sensitivities against ADCC.

Preparation of Transfectant Target Cells with Varying Expression Levels of Exogenous Antigen. To establish a simpler system for the investigation of the influence of the antigen amount on tumor cells independently from different cellular backgrounds, we next constructed panels of transfectant tumor cell lines with wide ranges of antigen expression levels. We used two antigen-specific systems for this aim, CCR4 and CD20. In addition to anti-CD20 IgG1s described above, two fucose variants of chimeric anti-CCR4 IgG1s have also been generated: the conventional highly fucosylated anti-CCR4 IgG1, KM3060, and its low-fucose counterpart, KM2760 (Table 1). They share identical amino acid sequences and CCR4 binding activities, whereas KM2760 has shown enhanced ADCC against $CCR4^+$ T leukemia cells (18).

Panels of target cells with a range of expression levels of the chosen antigens were constructed by transfecting *CCR4* or *CD20* genes into murine thymoma EL4 cells. EL4 cells were chosen as the host cell to generate target cells for the quantitative evaluation of ADCC because of their resistance to antibody-independent cytotoxic activity of human NK cells that could obscure antibody-dependent cytotoxicity. Following single cell cloning, eight CCR4-positive clones (designated CCR4/EL4-A to CCR4/EL4-H) and seven CD20-positive clones (CD20/EL4-A to CD20/EL4-G) were screened by nonquantitative flow cytometry as illustrated in Fig. 2. To generate high expressing $CD20^+$ clones, gene amplification in the presence of MTX was used: CD20/EL4-D and CD20/EL4-F were produced using 200 nmol/L MTX selection and CD20/EL4-G was produced using 1,000 nmol/L MTX.

The numbers of antibody binding sites per cell on each established EL4 clones were then determined using quantitative flow cytometry method and ranged from 1.3×10^3 to 5.4×10^4 for CCR4 and from 1.2×10^4 to 5.8×10^5 for CD20 (Table 2). All clones were confirmed to have similar cell diameters by flow cytometry (data not shown), implying that antigen densities on the surface of each target cell were expected to be proportional to the numbers of antibody binding sites shown in Table 2. Although the parent murine EL4 cell would not be expected to express human antigens and no visible staining were observed in nonquantitative flow cytometry (Fig. 2), the methodology used calculated ~600 sites per cell for each of the antigens. This was probably because of the marginal nonspecific or cross-reactive staining in the quantitative flow cytometry analysis. It should be noted that the CCR4 expression levels of all the human T-cell leukemia cell lines that we have previously described (18) ranged between those of CCR4/EL4 clone A and clone G used in these studies, as observed in nonquantitative flow cytometry (data not shown). CD20 expression on clinical B lymphoma cells has been reported to be $\sim 10^5$, although it depends on the clinical subtype of the lymphoma to some extent (3, 28–30). Taken together, the expression levels of the target cell clones established in this study were considered to be representative of the *in vivo* expression levels of patient's tumor cells.

Antibody-Dependent Cellular Cytotoxicity of IgG1 Fucose Variants against Experimental Target Cells with Various Antigen Expression Levels. We next measured the ADCC of both IgG1 fucose variants upon the experimental target cell lines described above. As shown in Fig. 3, using PBMC from peripheral blood of two healthy donors (donor A and B) as effector cells, the low-fucose KM2760 showed higher ADCC activity than that of the high-fucose KM3060 against each of the CCR4-transfected target cells. Analysis of the ADCC activity of the two IgG1s were each found to fit to a sigmoid-shaped curve with different maximal levels of cytotoxicity for

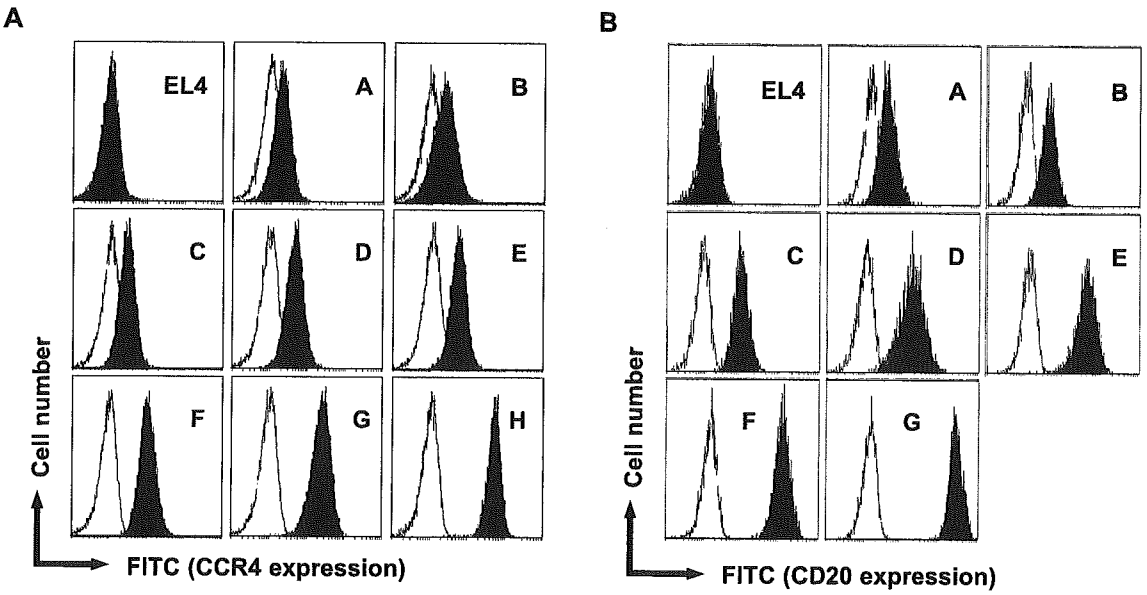

Fig. 2 Relative antigen expression levels in the established target cell clones. The parental EL4 cells and the clones with various expression levels of exogenous human *CCR4* (*A*) or *CD20* (*B*) genes were stained with biotynylated KM2760 or FITC-conjugated anti-CD20 monoclonal antibody, respectively. For CCR4-expressing clones, cells were washed and then stained with avidin-conjugated FITC as the secondary reagent. The stained cells (*filled histograms*) and the reference unstained samples (*blank histograms*) were then analyzed by flow cytometry. Clone names are indicated in each panel: A to H in *A*, clone CCR4/EL4-A to CCR4/EL4-H; A to G in *B*, clone CD20/EL4-A to CD20/EL4-G.

Table 2 Numbers of binding sites on the established target cell clones

CCR4-positive clones		CD20-positive clones	
Clone	Binding sites*	Clone	Binding sites†
CCR4/EL4-A	1.3×10^3	CD20/EL4-A	1.2×10^4
CCR4/EL4-B	1.6×10^3	CD20/EL4-B	1.5×10^4
CCR4/EL4-C	2.6×10^3	CD20/EL4-C	2.5×10^4
CCR4/EL4-D	4.6×10^3	CD20/EL4-D	4.1×10^4
CCR4/EL4-E	5.8×10^3	CD20/EL4-E	6.7×10^4
CCR4/EL4-F	1.5×10^4	CD20/EL4-F	2.1×10^5
CCR4/EL4-G	1.7×10^4	CD20/EL4-G	5.8×10^5
CCR4/EL4-H	5.4×10^4		
EL4	6.6×10^2	EL4	6.1×10^2

*Number of CCR4 binding sites per cell determined by quantitative flow cytometry.

†Number of CD20 binding sites per cell determined by quantitative flow cytometry.

the different IgG1s calculated by the four-parameter regression equations (Table 3). In addition, the minimum amount of antigen that was required to induce detectable level of ADCC of KM2760 was less than that of KM3060. For example, with donor A effector cells, KM2760 exhibited ADCC against all CCR4-expressing clones ($\geq 1.3 \times 10^3$ CCR4 binding sites), whereas KM3060 required at least 1.5×10^4 CCR4 binding sites in the presence of 3 μg/mL IgG1s (Fig. 3, *top right*). Further, we calculated the number of CCR4 binding sites required to achieve the half-maximal cytotoxicitiy of KM3060 for both KM2760 and KM3060 (Table 3). For example, with PBMC from donor A and 3 μg/mL antibody concentration, KM3060 required 2.1×10^4 CCR4 binding sites on target cells for its half-maximal cytotoxicity (14.4%), whereas KM2760 required only 9.6-fold less antigen to achieve the same level of cytotoxicity, indicating KM2760 required only approximately one tenth of CCR4 expression than KM3060 in this experimental condition. Similar quantitative relationships in the ADCC of the two IgG1s were observed in all cases in Fig. 3 except for a little smaller difference in efficacies of the two IgG1s (5.6-fold) with donor A PBMC and 0.1 μg/mL antibody concentration.

A similar advantage of low-fucose IgG1 in the lysis of low-antigen-expressing cells and the maximal cytotoxicity was also observed for CD20 system using PBMC from two other donors (Fig. 4), indicating that low-fucose IgG1 can reduce the antigen number required for ADCC in CD20 system in addition to increasing the maximal ADCC achievable. However, the shifts in required antigen amount was somewhat less compared with CCR4 system (the low-fucose KM3065 required ~3-fold less CD20 amount than rituximab in each experimental condition; Table 4). This may be due to the relatively higher ADCC mediated by the high-fucose IgG1 (rituximab). We also investigated another important Fc-mediated function of antibody, CDC, of the two anti-CD20 IgG1s on the CD20-transferred target clones (Fig. 5). In contrast to ADCC, the cytotoxicities of the two IgG1s were not significantly different. The anti-CCR4 IgG1s did not exhibit any measurable CDC activity against any of the CCR4-transfected target cells irrespective of their fucose contents (data not shown). These differing results between CCR4 and CD20 might be due to many factors including the expression levels of the antigens, the inherent capacity of the antigens to mediate CDC, or the antigen-binding affinity of individual antibody clone.

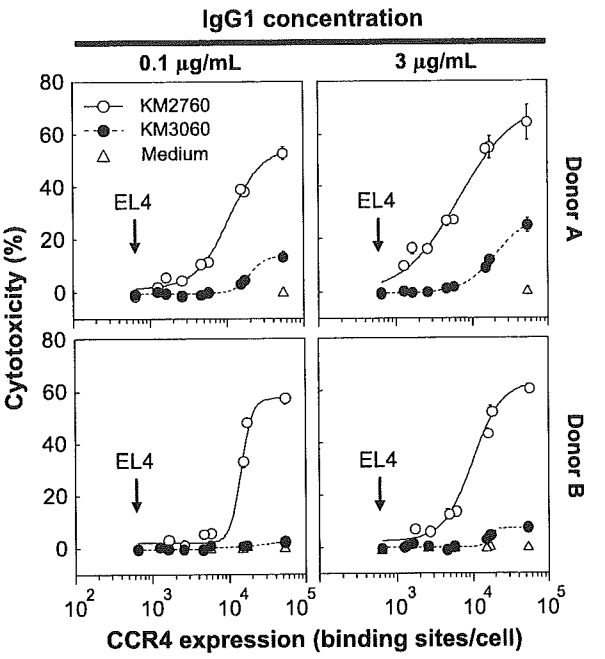

Fig. 3 ADCC of anti-CCR4 IgG1 fucose variants using EL4 transfectant clones with differing antigen expression as target cells. *Y*-axis, cytotoxicities in the presence of anti-CCR4 IgG1s or medium alone determined by 4-hour ^{51}Cr release assays. *X*-axis, number of CCR4 binding sites per cell of each target clone including parent EL4 cells (*arrows*). PBMC from healthy blood donors were used as effector cells, with a constant effector-to target ratio of 25:1. Two different PBMC donors (*donor A* and *donor B*) and IgG1 concentrations (0.1 and 3 μg/mL) were used as indicated.

Natural Killer Cell Binding of IgG1 Fucose Variants. The mechanism responsible for ADCC enhancement by fucose removal from IgG1 is an increase of IgG1 binding to FcγRIIIa (16, 27). This enhancement also results in effective ADCC at a lower antigen density. We have previously shown the improved FcγRIIIa affinity of KM3065 compared with rituximab by ELISA method (31) and determined the kinetic and thermodynamic parameters of the interaction between FcγRIIIa and the two anti-CD20 IgG1s (27). The enhanced FcγRIIIa binding by fucose removal was also confirmed for anti-CCR4 IgG1s (data not shown).

Table 3 Parameters in ADCC plots of anti-CCR4 antibodies

Donor	Antibody	Concentration (μg/mL)	Maximal lysis* (%)	EC_{50} (KM3060†; binding sites)	Ratio
A	KM3060	0.1	13.6	1.98×10^4	×5.6
	KM2760	0.1	55.0	0.36×10^4	
	KM3060	3	28.8	2.13×10^4	×9.6
	KM2760	3	71.8	0.22×10^4	
B	KM3060	0.1	5.66	7.67×10^4	×11
	KM2760	0.1	57.3	0.70×10^4	
	KM3060	3	7.37	1.63×10^4	×9.2
	KM2760	3	63.2	0.18×10^4	

*Estimated by using the four-parameter regression equations.

†Number of CCR4 binding sites per cell required to achieve the half-maximal lysis by KM3060.

Furthermore, the binding of IgG1 fucose variants to purified NK cells prepared from blood of one healthy donor was measured by flow cytometry (Fig. 6). The low-fucose anti-CCR4 and anti-CD20 IgG1s each showed slightly higher binding to NK cells than their highly fucosylated counterparts, which was consistent with the result of other analyses (16). Next, we examined whether IgG1 binding to NK cells was enhanced when anti-CCR4 IgG1 was ligated with clustered antigen (BSA-conjugated CCR4 peptide) to imitate the physiologic condition in which FcγRIIIa molecules on NK cells are cross-linked by the complex of antibody and target cells. Under these conditions, binding to NK cells was further enhanced for each antibody; however, the increase was greater for the low-fucose KM2760.

Antigen-Specific Natural Killer Cell Activation. To investigate whether increased binding of low-fucose IgG1 to FcγRIIIa and NK cells is a key step for NK cell activation during ADCC, we next investigated expression pattern of the activation marker CD69 on $CD56^+$ NK cells in the presence of both anti-CD20 IgG1 and four of the target cell clones with differing CD20 expression levels (EL4, CD20/EL4-C, CD20/EL4-E, and CD20/EL4-G; the numbers of CD20 binding sites per cell of each clone were shown in Table 2). The control experiment was first done by stimulating purified NK cells in the presence of phorbol 12-myristate 13-acetate and ionomycin for 24 hours to confirm the up-regulation of CD69 in whole population of NK cells (Fig. 7*A*).

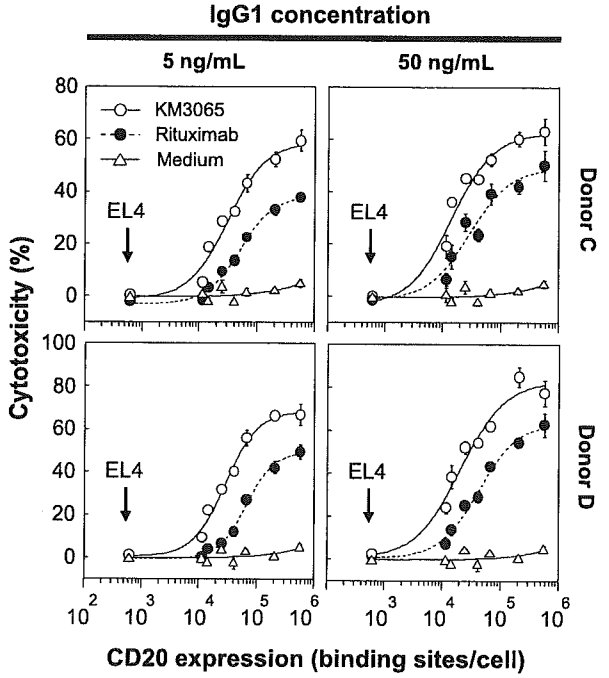

Fig. 4 ADCC of anti-CD20 IgG1 fucose variants using EL4 transfectant clones with differing antigen expression as target cells. *Y*-axis, cytotoxicities in the presence of anti-CD20 IgG1s or medium alone determined by 4-hour ^{51}Cr release assays. *X*-axis, number of CD20 binding sites per cell of each target clones including parent EL4 cells (*arrows*). PBMC from healthy blood donors were used as effector cells, with a constant effector-to target ratios of 25:1. Two different PBMC donors (*donor C* and *donor D*) and IgG1 concentrations (5 and 50 ng/mL) were used as indicated.

Table 4 Parameters in ADCC plots of anti-CD20 antibodies

Donor	Antibody	Concentration (ng/mL)	Maximal lysis* (%)	EC_{50} (rituximab†; binding sites)	Ratio
C	Rituximab	5	38.3	5.62×10^4	×3.0
	KM3065	5	58.8	1.88×10^4	
	Rituximab	50	49.2	2.99×10^4	×2.7
	KM3065	50	62.7	1.10×10^4	
D	Rituximab	5	49.2	6.70×10^4	×3.4
	KM3065	5	68.2	1.99×10^4	
	Rituximab	50	63.3	4.12×10^4	×3.2
	KM3065	50	83.2	1.30×10^4	

*Estimated by using the four-parameter regression equations.
†Number of CD20 binding sites per cell required to achieve the half-maximal lysis by rituximab.

When mixed with the EL4-derived target cells, NK cells could be clearly identified and removed from the flow cytometeric analysis due to their relative small diameter reflected in forward scatter (Fig. 7*B*); accordingly, CD56/CD69 expression levels in NK cells mixed with target cells for 4 and 24 hours were analyzed in the absence or presence of various antibodies (KM3065, rituximab, or anti-CCR4 KM2760 as an irrelevant control antibody; Fig. 7*C*). In the absence of antibody, no CD69 up-regulation was observed either at 4 or 24 hours (Fig. 7*C*, *medium column*), which was consistent with the resistance of the EL4 clones to antibody-independent cytotoxicity observed in the ADCC assays (Figs. 3 and 4).

In the presence of CD20-positive target cells at 4 hours, the two anti-CD20 IgG1s each increased the proportion of activated NK cells in a manner dependent on CD20 expression level. The low-fucose anti-CD20 antibody, KM3065, consistently induced higher numbers of activated NK cells than rituximab: 36% to 45% activation of NK cells for KM3065 versus 8% to 22% for rituximab. At 24 hours, KM3065 activity was increased, but no longer obviously antigen-density dependent, with activation of majority of NK cells (64-71%) irrespective of CD20 expression levels on target cells. With rituximab at 24 hours, the activation was also significantly increased from 4-hour incubation (24-48%), although still lower than that with KM3065, and increased at higher antigen density. NK cell activation by both IgG1s were considered maximal at this time point because the CD69-positive NK cell proportions in the presence of anti-CD20 IgG1s at 24 hours was unchanged when the incubation time was extended to 48 hours (data not shown). Taken together, these results provide evidence of a possible mechanism by which low-fucose IgG1 can increase ADCC on target cells with low antigen expression, namely activation of more NK cells by low fucose antibodies than conventional high-fucose IgG1.

When mixed with CD20-negative EL4 cells and anti-CD20 IgG1, or when mixed with CD20-positive cells and irrelevant IgG1 KM2760, NK cells did not exhibit up-regulated CD69 expression at any time during the experimental period. These results indicate the strict dependency of low-fucose IgG1 in mediating ADCC on the presence of antigen, despite its antigen-independent binding capacity to NK cells as shown in Fig. 6.

There are two distinct subsets of human NK cells identified by cell surface density of CD56: a small population of $CD56^{bright}$ (<10%) and the remainder $CD56^{dim}$ (32). To identify which population was involved in anti-CD20 IgG1-mediated NK cell

activation, the flow cytometer histograms obtained above were reanalyzed according to CD56 expression on NK cells. As a result, no apparent increase in CD69 expression in $CD56^{bright}$ subset was observed in all the samples shown in Fig. 7*C*, suggesting that the NK cell subset responsible for ADCC mediated by both the IgG1 fucose variants was $CD56^{dim}$. An example is shown in Fig. 7*D*, 24-hour incubation in the presence of CD20/EL4-E.

DISCUSSION

One of the major obstacles to optimizing the efficacy of therapeutic antibodies is low and heterogeneous antigen expression that (*a*) allows cells to evade the effective treatment, (*b*) induces the selection of low antigen cell, and (*c*) makes some antigenic targets resistant to antibody therapeutics. For example, the most successful anticancer antibody, rituximab, shows an inferior clinical response rate for lymphoma subtypes that have a relatively lower expression of CD20, such as chronic lymphocytic leukemia or small lymphocytic lymphoma, compared with highly responsive follicular lymphoma with higher CD20 expression, although it should be noted that other factors such as the differential expression of complement-inhibitory proteins (CD46, CD55, CD59) among these clinical subtypes might also affect the rituximab responsiveness (3). It has been shown that antigen expression is a critical factor of the efficacy of the anti-HER2 IgG1 trastuzumab (1, 2, 4, 33), for which treatment is restricted to HER2-overexpressing 20% to 30% breast cancer patients as determined by immunohistochemistry or fluorescence *in situ* hybridization before therapy (34). Trastuzumab-mediated ADCC, considered a critical therapeutic mechanism of the antibody, is dependent on the levels of HER2 on target cells: The antibody can induce ADCC only against tumor cells with $\geq 10^5$ HER2 molecules per cell (35, 36). In addition, residual tumor cells with lower antigen expression could escape from antibody therapy, which might lead to relapse and resultant poor prognosis. As the problem of the low or heterogeneous antigen expression on target cells is relevant for many other therapeutic antibodies, enhanced ADCC due to the augmentation of low-fucose IgG1 binding to FcγRIIIa is a promising way to address this problem.

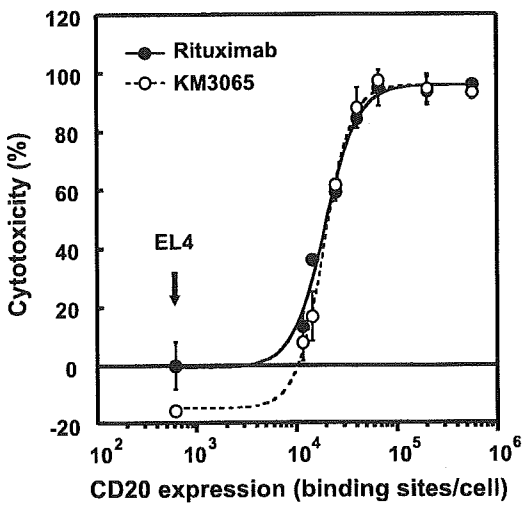

Fig. 5 CDC of anti CD20 IgG1 fucose variants against clones with differing CD20 expression as the target cell. IgG1 concentration used was 1 μg/mL. CDC against parent EL4 cells is also shown (*arrow*).

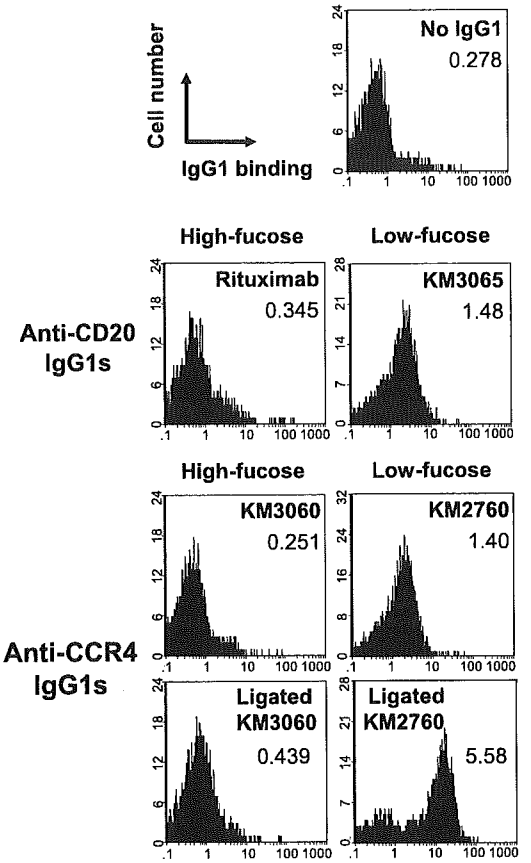

Fig. 6 NK cell binding of IgG1 fucose variants by flow cytometry. Antibodies used to stain NK cells and mean fluorescence intensity values are indicated. In some experiments, anti-CCR4 IgG1s were ligated with BSA-conjugated CCR4 peptide (20 μg/mL) by the 10-minute preincubation of IgG1s and the conjugate on ice. Data are representative of two repeat experiments.

Previous studies have only shown the enhanced ADCC of low-fucose IgG1 upon target cell lines with a fixed and relatively high density of antigen (16–18). How the antigen expression of target cells modulates the advantage by fucose reduction on ADCC remained unanswered. To investigate whether low-fucose IgG1 could exhibit potent ADCC on target cells with less antigen amount, we constructed panels of target cells with a range of known antigen expression levels. Because the obtained clones were uniform in their cell diameters and susceptibilities to antigen-independent lysis by NK cells, the use of these experimental target cells enabled the measurement of the dependence of ADCC activity on antigen amount, and hence density, per target cell. Interestingly, antigen amount required for ADCC induction for low-fucose IgG1 was lower than that for high-fucose IgG1, suggesting that improvement of IgG1 binding to FcγRIIIa on effector cells by fucose depletion can reduce antigen amount necessary for ADCC induction. Because the antigen-binding activities do not vary among fucose variant IgG1s and consequently the IgG1 amount bound on the surface

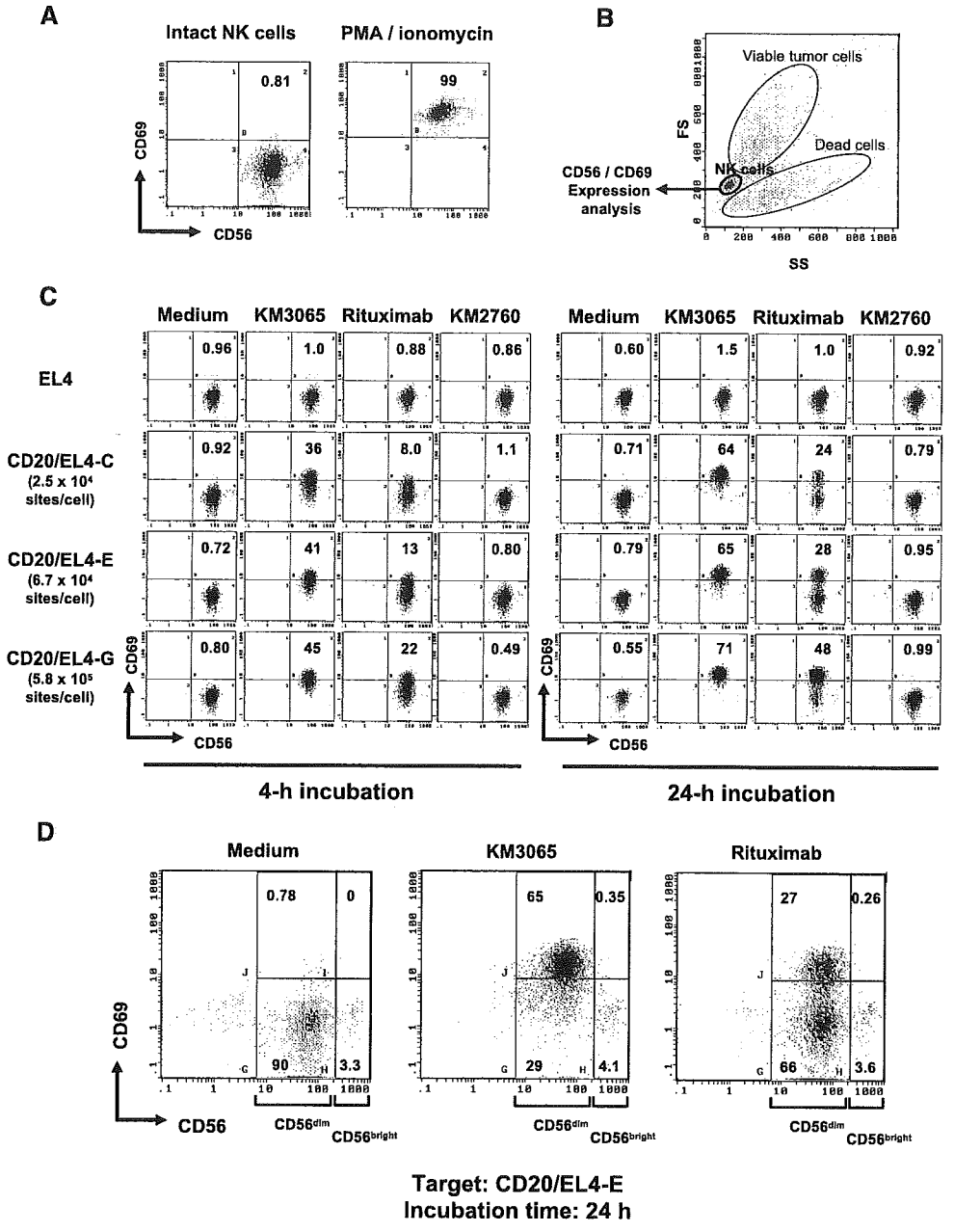

Fig. 7 NK cell activation during ADCC analyzed by flow cytometry. Figures show the proportion (%) of $CD56^+CD69^+$ cells. *A*, NK cells purified from PBMC using MACS displayed $CD56^+CD69$ and phenotype (*left*). After control stimulation in the presence of phorbol 12-myristate 13-acetate and ionomycin for 24 hours, 99% of the cells had up-regulated surface CD69 expression. *C*, analysis of CD69 expression on NK cells in the presence of target cells and antibodies. One hundred thousand NK cells and an equal number of the indicated target cells were mixed in a round-bottomed 96-well plate in the presence of the indicated IgG1 at the final concentration of 1 μg/mL or medium alone. After incubation for 4 hours (*left*) or 24 hours (*right*), cells were harvested and subjected to CD69/CD56 expression analysis. The cytograms are the CD69/CD56 expression of NK cells gated out from the whole cell mixture by their relatively small forward scatter/side scatter value (*B*). Figures show the percentage of $CD56^+CD69^+$ cells. *D*, an example of the reanalysis of NK cells according to their CD56 density. $CD56^+$ compartment was further divided into $CD56^{dim}$ and $CD56^{bright}$ populations. Figures show the percentage of the cell in each analyzed compartment.

of target cells were unaffected by fucose content in IgG1 as confirmed by flow cytometry (data not shown), the potent ADCC induction by low-fucose IgG1 might be due to the efficient activation of effector cells via more effective interactions with FcγRIIIa even in the presence of low IgG1 density on target cells.

Although we did not investigate *FCGR3A*-158 genotype of the PBMC donors in the current studies, *FCGR3A*-158V/F polymorphism is also likely to affect the antigen density required for ADCC because our data imply that IgG1-FcγRIIIa affinity affects the antigen density threshold required for ADCC induction. However, fucose depletion is expected to lower the required antigen density for any PBMC donors because it improves IgG1-FcγRIIIa binding independently of the *FCGR3A* genotypes (31), although the difference in required antigen

densities between IgG1 fucose variants may vary with the *FCGR3A* genotype.

Although reduction of fucose showed the benefits of ADCC induction in low antigen density for both CCR4 and CD20 specificities, the CCR4 system displayed a more marked difference between ADCC of fucose variants than CD20 system. Possible explanations for this difference include the following: The higher amount of CD20 on the experimental target cells (approximately one order of magnitude higher than CCR4; Table 2) might be enough for the ADCC induction of high-fucose IgG1. Alternatively, the inherent structures of each antigen molecules, especially the mobility and the configuration of the molecules in lipid bilayer on cell surface, might affect the efficacy of high-fucose IgG1. In contrast to CCR4, which is a seven-transmembrane-spanning G-coupled receptor (37) and is presumed to have poor mobility in lipid bilayer, CD20 is highly mobile and naturally forms multimer (38–40). In addition, most of anti-CD20 antibodies including rituximab can redistribute CD20 into lipid rafts, which determines the capacity to induce strong CDC (41). Although the relation of ADCC and the redistribution into lipid rafts has been poorly defined, high density of IgG1 bound on CD20 multimer or localized CD20 in lipid rafts may induce ADCC even by high-fucose IgG1. The hypothesis that clustering IgG1 could enhance ADCC is supported by the reports of dimerized antibodies having potent ADCC (42, 43).

As expected from the identical binding capacities of fucose variant IgG1s to C1q (16), KM3065 and rituximab did not vary in their CDC activities against the target cell clones with varying antigen expression. Although the anti-CD20 IgG1s exerted CDC even upon low or intermediate $CD20^+$ clones, whose antigen expression levels overlapped with those of higher CCR4 expressing clones, anti-CCR4 IgG1s did not mediate detectable CDC activity against all $CCR4^+$ clones. This discrepancy may again support the hypothesis that CCR4 and CD20 might differ in their inherent properties of the molecule, such as clustering capacity in lipid bilayer, which is critical for CDC susceptibility (41) and possibly affect the susceptibility to high-fucose IgG1-mediated ADCC shown in Fig. 4. Because the low-fucose anti-CCR4 IgG1 greatly augmented the ADCC of high-fucose anti-CCR4 IgG1, the inability of anti-CCR4 antibody to mediate CDC also implies the therapeutic benefit of low-fucose IgG1 that it would be applicable for wider range of molecular targets where CDC cannot be expected due to inherent molecular properties of the antigen.

We further investigated the mechanism of enhanced ADCC by low-fucose IgG1 in terms of NK cell activation. Consistent with the ADCC analysis, KM3065 induced more CD69-positive activated NK cells than rituximab even in the presence of lower antigen density, suggesting that low-fucose IgG1 can efficiently recruit and activate effector cells via the increased binding to FcγRIIIa. The activated NK subset was predominantly $CD56^{dim}$, a not unexpected finding because $CD56^{bright}$ NK cells express low level of FcγRIIIa and are presumed to function as cytokine responder/producer cells rather than cytotoxic killer cells (30, 44–46). Further, NK cells were shown to be activated only by IgG1 bound on target cells despite low-fucose IgG1 itself could bind slightly to NK cells in the absence of antigen (Fig. 6). This is a very important finding as it suggests that enhanced FcγRIIIa/NK interactions should not induce nonspecific side effects. The mechanism of the tumor-specific activation of NK cells via low-fucose IgG1 remains unknown; however, it may be that intracellular signals through FcγRIIIa are not triggered until the density of receptor-bound IgG1 is elevated above a minimal level by antigen molecules present on target cells. Enhanced binding of low-fucose IgG1 to FcγRIIIa might lower the threshold of IgG1 density on target cells necessary for NK cell activation and consequently results in ADCC induction against targets with fewer antigen molecules. This hypothesis is supported by the results herein that low-fucose IgG1 binding was greatly enhanced by preligating the antibody with antigen to mimic cell-surface antigen-antibody clusters increase NK cell binding at concentration of highly fucosylated IgG1 did not bind (Fig. 6).

In conclusion, our data showed that low-fucose IgG1 shows potent ADCC upon target cells with lower antigen density compared with conventional antibodies, through the effective and antigen-specific activation of NK cells due to augmented binding to FcγRIIIa. These features of low-fucose IgG1 could be therapeutically beneficial because clinical tumors often display the heterogeneity in their antigen expression levels and in addition the number of effector cells accessible to *in vivo* tumor would be fewer compared with *in vitro* experimental condition.

ACKNOWLEDGMENTS

We thank Dr. Philip Wallace for helpful suggestions and critical reading of the manuscript.

REFERENCES

1. Carter P. Improving the efficacy of antibody-based cancer therapies. Nat Rev Cancer 2001;1:118–29.

2. Glennie MJ, van de Winkel JGJ. Renaissance of cancer therapeutic antibodies. Drug Discov Today 2003;8:503–10.

3. Smith MR. Rituximab (monoclonal anti-CD20 antibody): mechanisms of action and resistance. Oncogene 2003;22:7359–68.

4. Clynes RA, Towers TL, Presta LG, Ravetch JV. Inhibitory Fc receptors modulate *in vivo* cytoxicity against tumor targets. Nat Med 2000;6:443–6.

5. Cartron G, Dacheux L, Salles G, et al. Therapeutic activity of humanized anti-CD20 monoclonal antibody and polymorphism in IgG Fc receptor FcγRIIIa gene. Blood 2002;99:754–8.

6. Anolik JH, Campbell D, Felgar RE, et al. The relationship of FcγRIIIa genotype to degree of B cell depletion by rituximab in the treatment of systemic lupus erythematosus. Arthritis Rheum 2003;48: 455–9.

7. Weng WK, Levy R. Two immunoglobulin G fragment C receptor polymorphisms independently predict response to rituximab in patients with follicular lymphoma. J Clin Oncol 2003;21:3940–7.

8. Koene HR, Kleijer M, Algra J, von Roos D, dem Born AE, de Haas M. FcγRIIIa-158V/F polymorphism influences the binding of IgG by natural killer cell FcγRIIIa, independently of the FcγRIIIa-48L/R/H phenotype. Blood 1997;90:1109–14.

9. Wu J, Edberg JC, Redecha PB, et al. A novel polymorphism of FcγRIIIa (CD16) alters receptor function and predisposes to autoimmune disease. J Clin Invest 1997;100:1059–70.

10. Leget GA, Czuczman MS. Use of rituximab, the new FDA-approved antibody. Curr Opin Oncol 1998;10:548–51.

11. Gopal AK, Press OW. Clinical applications of anti-CD20 antibodies. J Lab Clin Med 1999;134:445–50.